EXTERNAL SULFATE ATTACK ON PORTLAND CEMENT INCORPORATING HIGH-VOLUME OF DOLOMITE POWDER PRE-CURED AT 20 °C AND 60 °C

DENG CHEN[1]* , LI-WU MO[2], AI-GUO WANG[3], KAI-WEI LIU[3], TAO YANG[4], SHI-PING ZHANG[5], FEI SONG[6]

[1.] *College of Civil Engineering, Suzhou University of Science and Technology, Suzhou 215011, China;*
[2.] *College of Materials Science and Engineering, Nanjing Tech University, Nanjing 211800, China;*
[3.] *Anhui Province Key Laboratory of Advanced Building Materials, Anhui Jianzhu University, Hefei 230601, China;*
[4.] *College of Materials Science and Engineering, Yancheng Institute of Technology, Yancheng 224051, China;*
[5.] *Department of Architecture Civil Engineering, Nanjing Institute of Technology, Nanjing 211167, China;*
[6.] *College of Materials Science and Engineering, Hunan University of Science and Technology, Xiangtan 411100, China)*

This work focuses on the sulfate resistance performances of Portland cement (PC) incorporating different amounts (0~60 wt%) of dolomite powder (DM) pre-cured at different temperatures (20 °C and 60 °C). The results show that the PC-DM samples pre-cured at 20 °C for 28 d and then eroded by sulfate solution for 180 d exhibit the worse appearances and higher expansion values than the reference PC sample. On the opposite, the sulfate resistance performances of the PC-DM samples pre-cured at 60 °C are better than those of the PC sample. Furthermore, with the increase of the DM content, the sulfate resistance properties get better and better. The degradation of the pore structure may act as a major factor for the poor sulfate resistance of the PC-DM samples pre-cured at 20 °C. However, for the PC-DM samples pre-cured at 60 °C, the poor pore structure does not increase the risk of sulfate erosion. This is mainly due to that the formation of hydrotalcite (Ht) results in the decomposition of monosulfate, and SO_4^{2-} may also be bound firmly by Ht in the PC-DM samples, thus contributing to the excellent sulfate resistance. Additionally, brucite can be identified in the PC-DM samples pre-cured at 60 °C, especially with high DM dosages (≥40 wt%).

Keywords: : *dolomite powder; sulfate attack; pore structure; hydrotalcite*

1. Introduction

External sulfate attack is a serious durability problem for cement-based materials, which describes a series of chemical and physical processes after contact of external SO_4^{2-} with cement matrix [1,2]. In the last few decades, severe damages have occurred in many concrete structures including dams, bridge piers and highway or railway tunnels around the world due to external sulfate attack [3-5]. Generally speaking, three primary strategies have been adopted to prevent sulfate attack including 1) limiting the C_3A content; 2) reducing the concrete permeability and 3) incorporating supplementary cementitious materials (SCMs) [6-10]. Among these, the incorporation of traditional SCMs such as fly ash, slag and silica fume can improve sulfate resistance significantly attributed to three different mechanisms [11]: a) reducing the C_3A content by decreasing the clinker content; b) consuming portlandite from cement matrix due to the pozzolanic reaction; c) improving the pore structure due to the better particle packing and pozzolanic reaction.

In recent years, the rapid growth of concrete materials consumption in all the word motivates the large requirements for SCMs. However, the supplies of traditional SCMs are becoming insufficient in most areas of the world due to the more strict environment protection policy [12-14]. Therefore, it is vital to explore a new kind of green and cheap SCM with excellent performance which can be applied in cement-based materials. Dolomite is a natural carbonate rock, which is abundantly available, widespread, inexpensive and similar to limestone in geological formation and microstructure [15,16]. Dolomite powder (DM) as a new SCM used in cement-based materials has attracted more attentions. Many studies [17-20] have demonstrated that the incorporation of DM can accelerate the hydration of Portland cement (PC), improving the workability and volume stability of cement-based materials. Similar to limestone powder (LS), DM also can react with C_3A to form the calcium carboaluminate including hemicarbonate (Hc) and monocarbonate (Mc), thus resulting in the stabilization of ettringite, which is beneficial to the strength development of cement-based materials [14,21,22]. However, unlike LS, Mg-Al hydrotalcite (Ht) may be formed in the PC-DM pastes cured at elevated temperature as a result of Mg released from DM, which is also deem to contribute to the strength development of cement-based materials [23,24]. Furthermore, several studies [25,26] have reported that DM has a positive effect on the durability of cement-based materials pre-cured at high temperature, such as good carbonation and chloride-permeation resistance, which is mainly due to that the formed Ht can bind effectively CO_3^{2-} and Cl^-. As is well known, sulfate attack resistance is crucial to the durability properties of concrete. Recent studies [27, 28] also revealed that the incorporation of 10~30 wt% DM can also improve the sulfate resistance properties of cement mortars pre-cured at high temperatures, even if the porosity increases

*Autor corespondent/*Corresponding author*,
E-mail: deng2928326@163.com

Table 1

Chemical compositions of materials (wt %)

	SiO_2	Fe_2O_3	Al_2O_3	CaO	MgO	K_2O	Na_2O	LOI
PC	22.18	5.76	3.98	62.47	0.87	0.85	0.10	2.28
DM	2.00	0.25	0.88	29.73	21.89	0.04	0.02	44.69

from 8.76% to 11.35% with the addition of 30 wt% DM.

At present, the large replacement of cement by traditional SCMs such as fly ash and slag has been conducted widely to reduce the carbon footprint of concrete and meanwhile improve the durability of concrete. However, the studies on DM addition are far from comprehensive. In previous studies, DM was used to replace up to 30 wt% of cement. Little works have been done on concrete durability when even higher additions (>50 wt%) of DM are added. In this paper, the sulfate resistance performances of PC incorporating 0~60 wt% DM pre-cured in water at 20 °C and 60 °C water for 28 d were investigated, respectively. The aim was to determine what's the effect of the addition of high-volume DM on the sulfate resistance of cement-based materials, especially pre-cured at high temperatures. To elucidate the effect mechanism, the deterioration products were analyzed by X-ray diffraction (XRD), the microstructure was appreciated by low-field nuclear magnetic resonance (LF-NMR) and backscatter scanning electron microscope (BSEM).

2. Experimental

2.1 Materials

In this experiment, Type P.II 52.5 PC was produced by China Cement Company in Jiangsu, China. DM was purchased from Yuyuan Mining Company in Hebei, China. The particle size distributions of PC and DM are given in Figure 1, and the mean particle sizes (d_{50}) are 12 μm and 6 μm, respectively. Table 1 shows the chemical compositions of PC and DM. The mineralogical compositions of DM were examined by using XRD (Rigaku Smartlab) with CuKα radiation. As is presented in Figure 2, DM mainly contains dolomite.

2.2 Methods

Blended cements were prepared with 0~60 % DM by weight, and the mix proportions are given in Table 2. All the pastes with a constant water/binder of 0.5 were cast in 20 mm × 20 mm × 20 mm moulds, and mortars were prepared with a constant water/binder/sand ratio of 0.5/1/3 in 25 mm × 25 mm × 280 mm moulds. All the pastes and mortars were stored in a standard curing room (95% RH and 20 °C) for 24 h, and then they were demoulded and pre-cured in water at 20 °C and 60 °C water for 28 d, respectively. Thereafter, all the samples were soaked in the curing boxes with

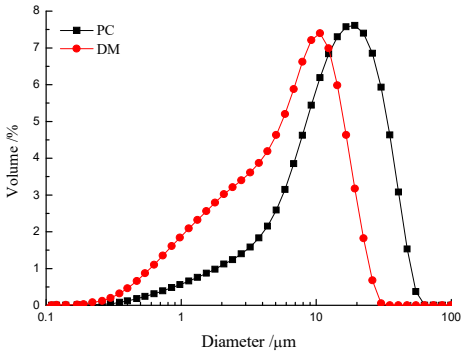

Fig. 1- Particle size distributions of PC and DM

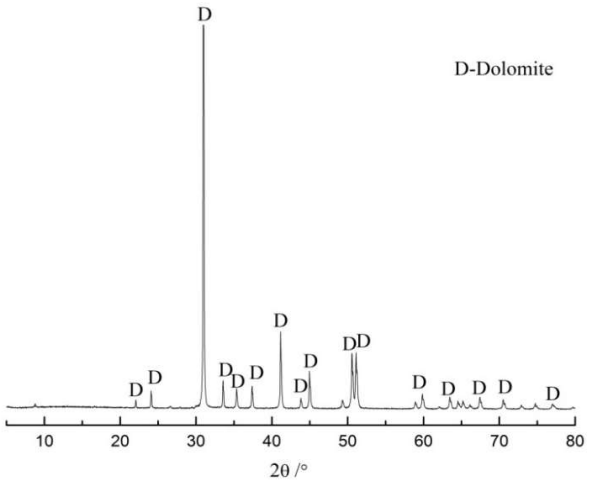

Fig. 2- XRD pattern of DM

Table 2

Compositions of blended cements (wt %)

ID	PC	DM
PC	100	0
PDC20	80	20
PDC40	60	40
PDC60	40	60

50 g/L sodium sulfate solution for 180 d at 20 °C. The appearance changes of cement paste samples and length changes of cement mortar samples were investigated after different ages of immersion in sulfate solution, respectively. For the length change test, a mean value of three cement mortar samples was used.

The cement pastes pre-cured for 28 d, were crushed and immersed in ethanol for 1 d to stop hydration, and then dried in a vacuum dryer for 1 d

at 40 °C. The pore structure of the samples was examined by using LF-NMR (MacroMR12-025V) according to references[29,30]. Meanwhile, the samples were also ground to pass by 80 μm mesh sieve for the analysis of hydration products with using XRD.

In order to investigate the erosion products changes, the samples of sulfate erosion for 180 d were cut with a liner precision to obtain the surface layer and inner core, as is shown in Figure 3. The surface layer and inner core of the samples were ground to a particle size < 80 μm, respectively, and the mineralogical compositions were determined by XRD. In addition, the inner cores of the samples were dried at 40 °C for 24 h, then impregnated with low-viscosity epoxy resin, carefully polished down to a surface roughness of 0.25 μm and examined by using BSEM (JSM-6150) with energy-dispersive spectrometer (EDS).

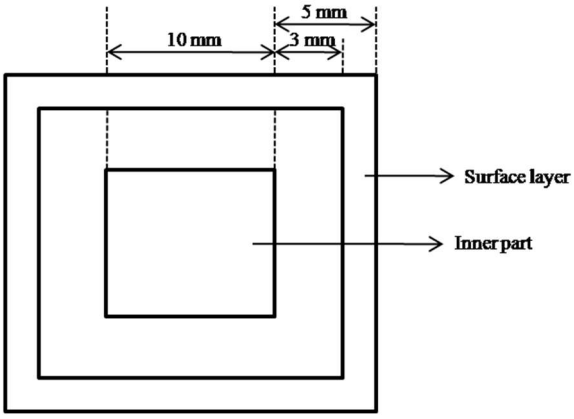

Fig. 3- The surface and inner portions of cement pastes for XRD analysis

3. Results and discussion

3.1 Appearance of cement pastes in sulfate solution

Figures 4 and 5 present the appearances of all the cement pastes pre-cured at 20 °C and 60 °C for 28 d, respectively. These pastes can achieve the high strengths by pre-curing in water at 20 °C and 60 °C water, and there are no cracks at the surfaces of these samples. Figure 6 shows the appearances of the paste samples pre-cured at 20 °C and then eroded by sulfate solution for 180 d. Due to the continuous penetration of external SO_4^{2-}, obvious cracks are formed at the edges of the PC sample. With the incorporation of DM, the samples immersed in sodium sulfate suffer more serious damages. Apparent spalling is occurred on the PC-DM samples, and the surface layer is completely separated, as can result in serious strength loss. It indicates that the incorporation of DM has an adverse effect on sulfate resistance of cement-based materials pre-cured at 20 °C.

In comparison to Figure 6, Figure 7 shows a slight damage at the corners and edges of the PC sample pre-cured at 60 °C. However, the blending with DM improves obviously the sulfate resistance, and no cracks are observed in the PC-DM samples. Moreover, the appearances of cement pastes become much better with increasing the DM content. It indicates that the elevated pre-curing temperature has a positive effect on the sulfate resistance of cement-based materials containing high-volume DM.

PC PDC20 PDC40 PDC60

Fig. 4- Appearances of cement paste samples pre-cured at 20 °C for 28 d

PC PDC20 PDC40 PDC60

Fig. 5- Appearances of cement paste samples pre-cured at 60 °C for 28 d

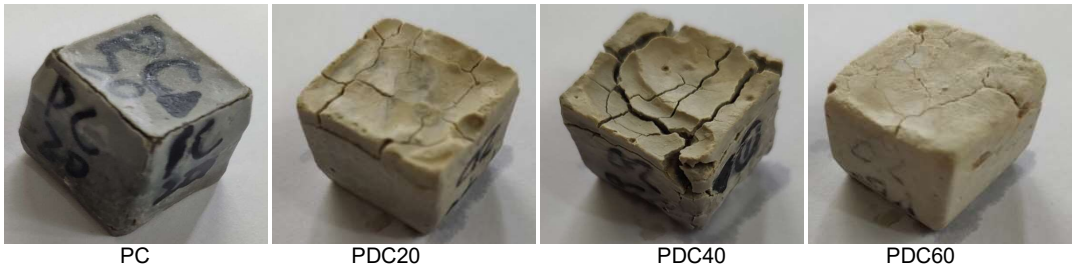

PC PDC20 PDC40 PDC60

Fig. 6- Appearances of cement paste samples pre-cured at 20 °C and then eroded by sulfate solution for 180 d

PC PDC20 PDC40 PDC60

Fig. 7- Appearances of cement paste samples pre-cured at 60 °C and then eroded by sulfate solution for 180 d

3.2. Expansion of cement mortars in sulfate solution

Figures 8 and 9 present the deformation trends of cement-mortars pre-cured at different temperatures for 28 d and then soaked in 20 °C 50 g/L sodium sulfate solution for up to 180 d.

As is shown in Figure 8, no obvious deformation is observed in the PC mortar at the ages from 0 to 28 d. As time goes on, the PC mortar sample develops a slow expansion at the ages from 28 to 90 d and a fast expansion after 90 d of immersion, which reaches 0.128% at 180 d. Blended cement mortars containing DM begin to expand after 7 d of immersion and the expansion increases continuously till 90 d. After 90 d, for the PDC20 and PDC40 mortars, the expansion trends are very similar and the expansion values reach 0.3385% and 0.395% at 180 d, respectively. For the PDC60 mortar, the expansion values are higher than those of the PDC20 and PDC40 mortars from 0 to 90 d, but the expansion values start to below those of the PDC20 and PDC40 mortars after 90 d. It may be due to that the incorporation of 60% DM reduces more C_3A content in cement, and the insufficient of aluminous phases in blended cement pastes mitigates a certain expansion in the later period.

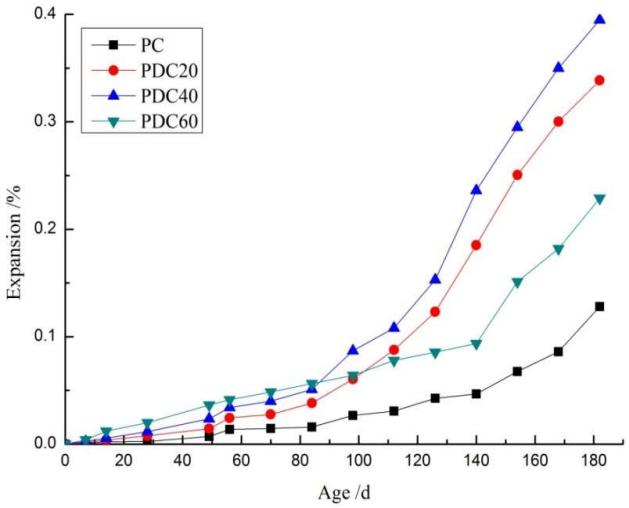

Fig. 8- Deformation of cement mortars pre-cured at 20 °C and then eroded by sulfate solution for different ages

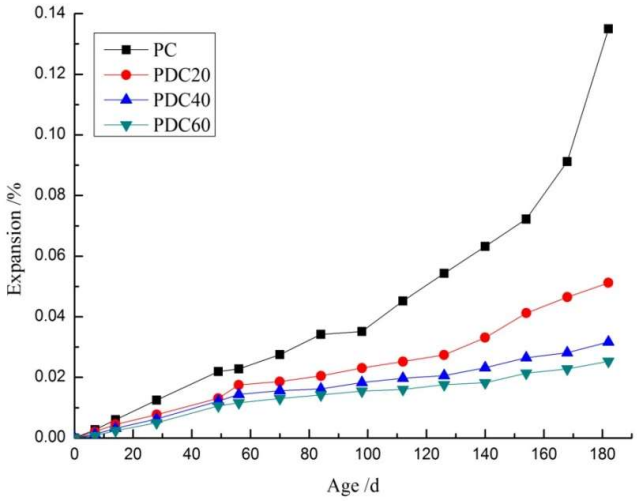

Fig. 9- Deformation of cement mortars pre-cured at 60 °C and then eroded by sulfate solution for different ages

3.3 Hydration products and pore structure of cement pastes pre-cured for 28 d

The XRD patterns which range from 8 to 22°2θ for all the cement pastes pre-cured at different temperatures for 28 d before sulfate attack are presented in Figures 10 and 11. At 20 °C, the main hydration products of the samples are ettringite, Hc, Mc and portlandite. It can be found obviously that the diffraction peak of Mc increases with the incorporation of DM into PC, and the higher the DM content, the higher the Mc peak. Additionally, no Hc is detected in the PDC40 and

PDC60 pastes, and the PC and PDC20 pastes still contain a slight amount of Hc. This suggests that the increasing content of DM may promote the conversion from Hc to Mc due to the additional CO_3^{2-} supplied by DM.

For samples pre-cured at 60 °C, Figure 11 shows that the hydration products differ from those at 20 °C. The ettringite, Hc and Mc are not found in the pastes because these phases are unstable when the temperature is 60 °C [31, 32]. For the PC paste, the diffraction peaks of monosulfate and portlandite are obviously. The monosulfate peak appears also, for sample with 20% DM and no monosulfate is observed in the PDC40 and PDC60 pastes. On the contrary, no Ht is found in the PC paste, and the Ht peak increases with increasing the content of DM. It seems that monosulfate transforms to Ht gradually with the increase of the DM amount in blended PC. A small diffraction peak of kilchoanite is found in the PC, PDC20 and PDC40 pastes; this may be due to the hydration of β-C_2S at high temperatures [33]. Additionally, the diffraction peak of brucite is observed in the PDC60 paste.

Figures 12 and 13 present the pore size distributions of all the cement pastes pre-cured at different temperatures for 28 d. In general, the pore with the diameter more than 0.1 μm is recognized as the harmful pore in cement-based materials [34]. According to Figure 12, it is clear that the increase of the DM content increases obviously the pore volume percentage of the large pores (>0.1 μm), indicating the incorporation of DM degrades the pore structure. Similarity, the pore structure of the cement pastes pre-cured at 60 °C is also coarsened remarkably by adding DM into PC, as is shown in Figure 13.

Figure 14 shows the total porosities of all the pastes pre-cured for 28 d. The porosities of the PC, PDC20, PDC40 and PDC60 pastes pre-cured at 20 °C are 27.94%, 31.08%, 34.65% and 38.8%, respectively. The porosities of the PC, PDC20, PDC40 and PDC60 pastes pre-cured at 60 °C are 29.32%, 31.97%, 35.31% and 39.67%, respectively. These results show that the total porosities of cement pastes increase with increasing the DM content and elevating pre-curing temperature.

3.4 Reaction products after sulfate erosion

Figure 15 shows the XRD patterns of the cement pastes pre-cured at 20 °C and then eroded by sulfate solution for 180 d. It can be found that there are no obvious differences in the phase compositions of the surface layer and inner part. In comparison to Fig. 10, the diffraction peaks of ettringite in all the cement pastes after immersion in sulfate solution increases significantly. Furthermore, for blended cement samples, with incorporation of 20~40 wt% DM, the peaks of ettringite increase more. However, the ettringite peaks in the surface layer and inner part of the PDC60 sample decrease slightly in comparison to those of the PDC20 and

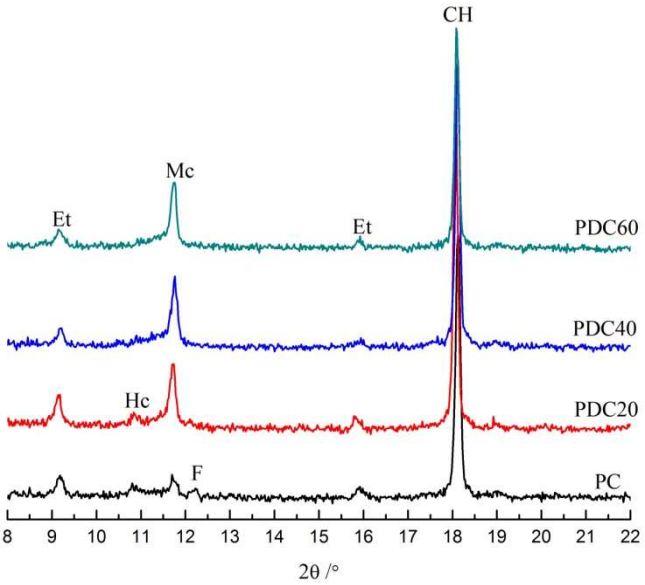

Fig. 10- XRD patterns of the pastes pre-cured at 20 °C for 28 d. CH: portlandite; Et: ettringite; F: ferrite; Hc: hemicarbonate; Mc: monocarbonate

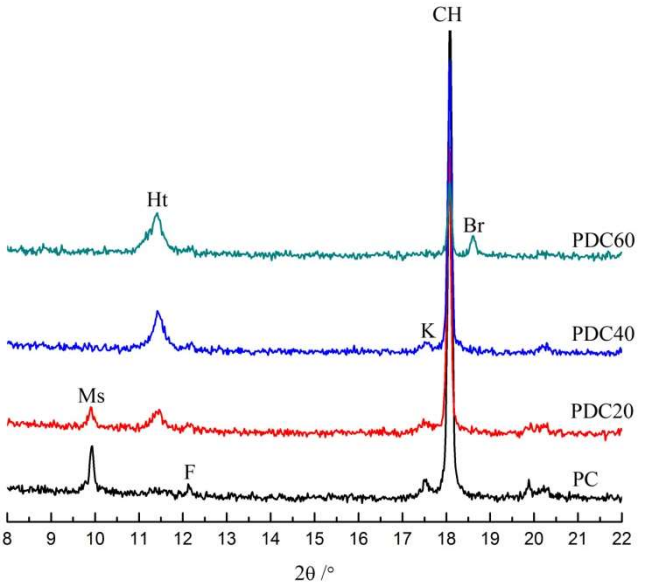

Fig. 11- XRD patterns of the pastes pre-cured at 60 °C for 28 d Br: brucite; CH: portlandite; F:ferrite; Ht: hydrotalcite; K: kilchoanite; Ms: monosulfate

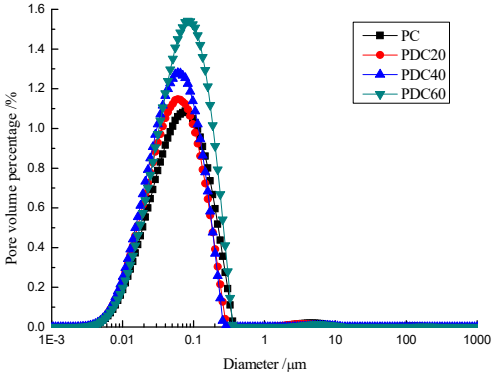

Fig. 12 - Pore size distributions of cement pastes pre-cured at 20 °C for 28 d

PDC40 pastes. In addition to ettringite, the peaks of gypsum are also detected at 2θ=20.8° obviously. On the opposite, the peaks of portlandite decrease gradually, with increase of DM content; especially no portlandite is found in the PDC60 sample. This is mainly due to that external SO_4^{2-} reacts with aluminous phases and portlandite in the cement pastes to increase the amount of ettringite and gypsum [2]. No Hc is observed in all the pastes. This may be attributed to that the formation of ettringite due to external sulfate attack also consumes calcium carboaluminate including Hc and Mc [27]. However, for the changes of the Mc content, it is difficult to distinguish of the main peak of Mc (11.7 °2θ) and gypsum (11.6°2θ).

Figure 16 shows the XRD patterns of the cement pastes pre-cured at 60 °C and then eroded by sulfate solution for 180 d. In comparison to Figure 11, for the PC paste, there is a major decrease in the diffraction peaks of monosulfate and portlandite in the surface layer and inner part, and the obvious peaks of ettringite and gypsum can be detected. However, the peaks of ettringite decreases with increasing the DM content, and no ettringite is observed in the PDC40 and PDC60 pastes. The peaks of gypsum are still obvious in the PDC20 and PDC40 pastes, but the relatively low peak of gypsum is only be detected in the surface layer of the PDC60 paste and no obvious gypsum can be found in the inner part. These results are the opposite of that of the PC-DM pastes pre-cured at 20 °C. Additionally, the diffraction intensities of Ht in the PDC20, PDC40 and PDC60 pastes are still higher, and a certain amount of brucite is found in the PDC40 and PDC60 pastes.

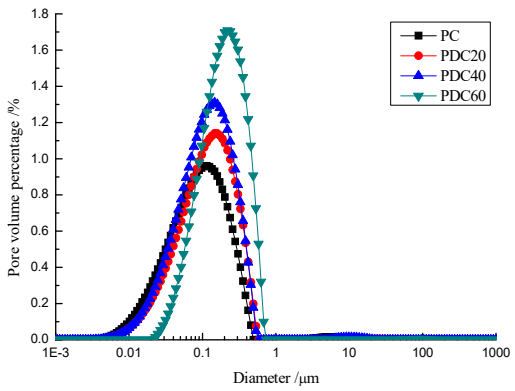

Fig. 13- Pore size distributions of cement pastes pre-cured at 60 °C for 28 d

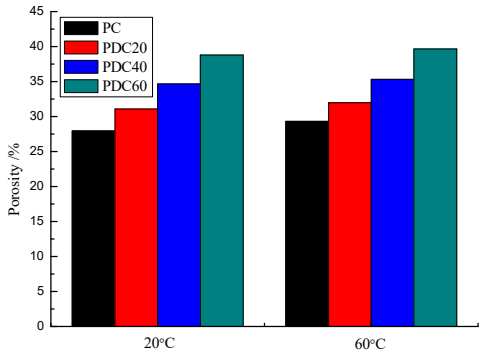

Fig. 14- Porosities of cement pastes pre-cured for 28 d

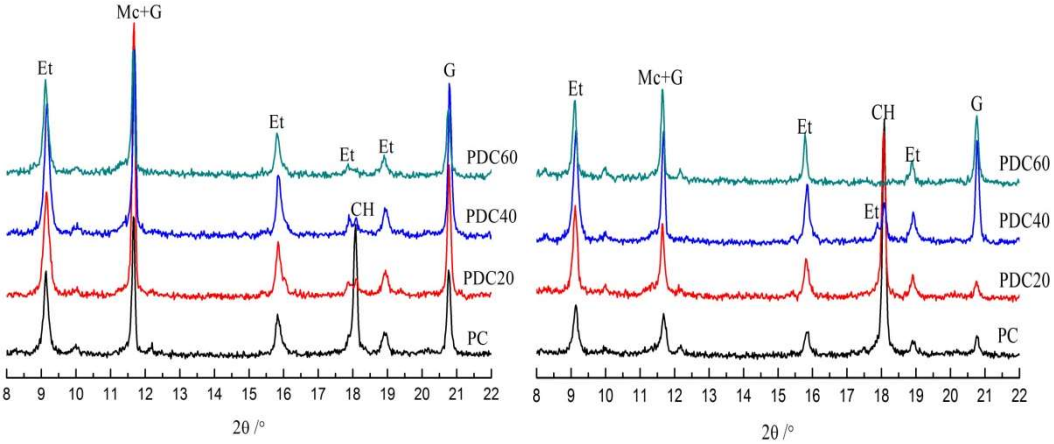

(a) Surface layer (b) Inner part

Fig. 15- XRD patterns of the cement pastes pre-cured at 20 °C and then eroded by sulfate solution for 180 d
CH: portlandite; Et: ettringite; G: gypsum; Mc: monocarbonate aluminate

3.5 Microstructure after sulfate erosion

Figure 17 shows the BSE images of the inner part of the PDC40 paste pre-cured at 20 °C and then eroded by sulfate solution for 180 d. As is shown in Figure 17(a), obvious cracks are observed in the inner part of the PDC40 paste, indicating that this sample is severely damaged by sulfate attack. Figure 17(b) shows the BSE image of the inner part at a magnification of × 4000, and lots of micro-cracks and pores are also visible. Figure 17(c) shows the EDS patterns of zone A. This zone is richen in Ca, Al, S and O. Combined with the XRD results in section 3.4, we can consider that the product in zone A is ettringite. Similarity, a large amount of ettringite is also found obviously in other positions of the inner core. The result corresponds

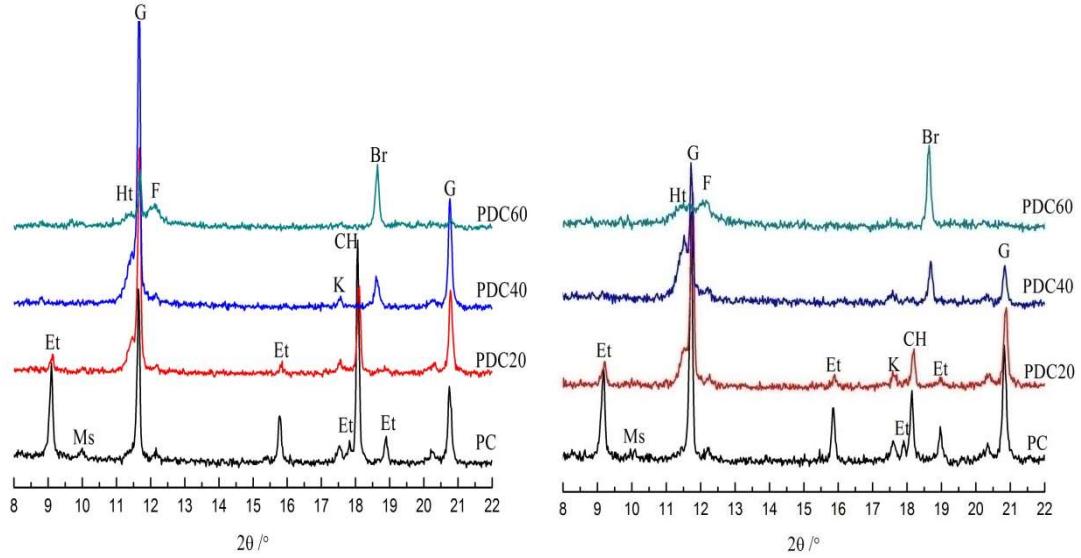

(a) Surface layer (b) Inner part

Fig. 16- XRD patterns of the cement pastes pre-cured at 60 °C and then eroded by sulfate solution for 180 d
Br: brucite; CH: portlandite; Et: ettringite; F:ferrite; G: gypsum; Ht: hydrotalcite; K: kilchoanite; Ms: monosulfate aluminate

to that of XRD analysis in section 3.4. In comparison to Figure 17, Figure 18 shows that no cracks can occur in the inner part of the PDC40 paste pre-cured at 60 °C. There is also no obvious ettringite in the inner part, indicating the elevated pre-curing temperature improves effectively the sulfate resistance of the PDC40 paste.

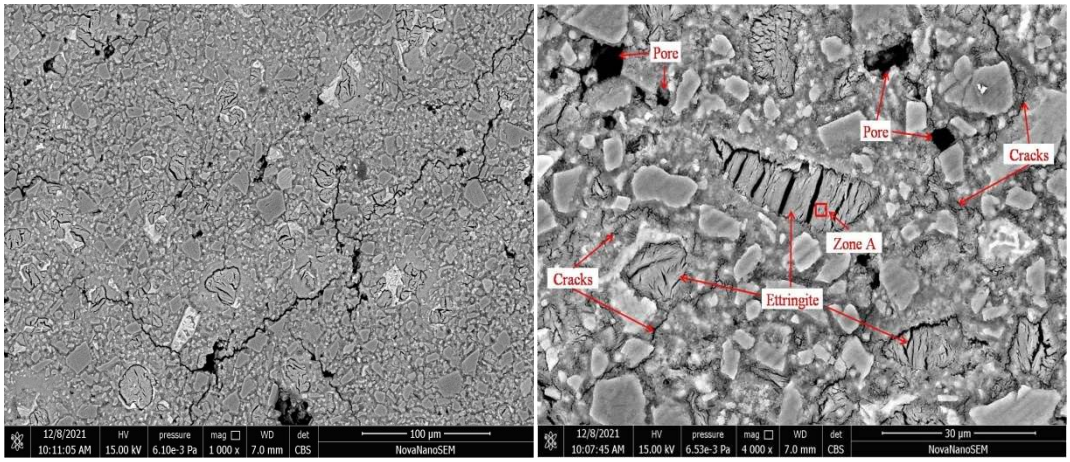

(a) 1000× (b) 4000×

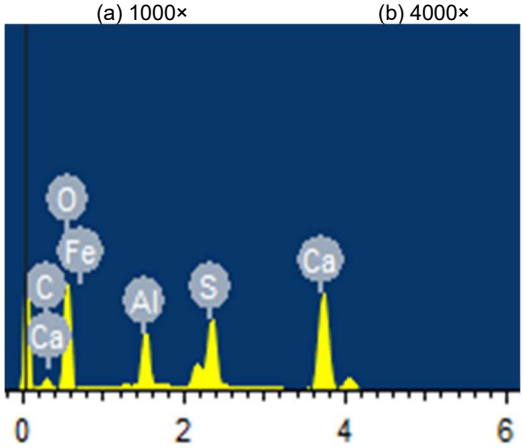

(c) EDS patterns of Zone A

Fig. 17- BSE images of the inner part of the PDC40 paste pre-cured at 20 °C and then eroded by sulfate solution for 180 d

•

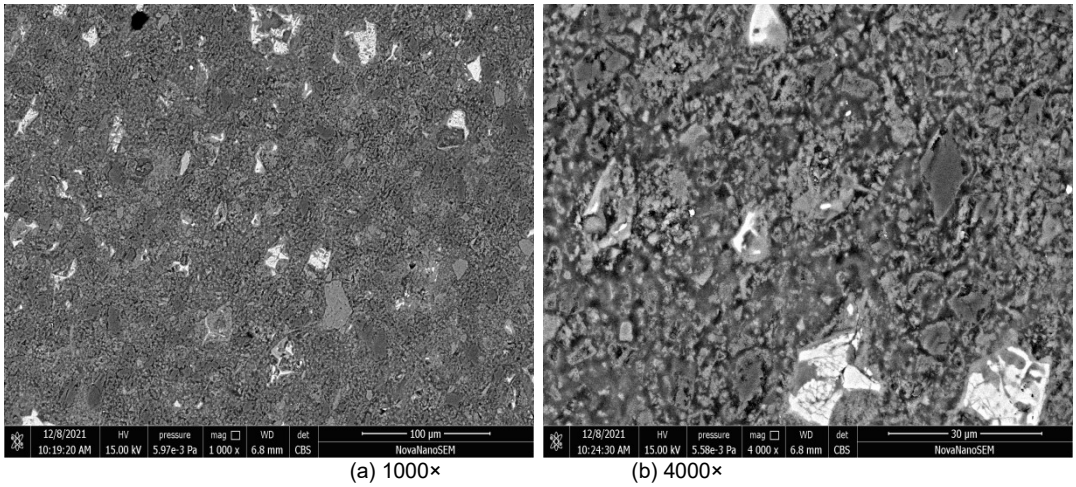

(a) 1000× (b) 4000×

Fig. 18- BSE images of the inner part of the PDC40 paste pre-cured at 60 °C and then eroded by sulfate solution for 180 d

3.6. Discussion

3.6.1 Sulfate resistance of cement-based materials pre-cured at 20 °C

As is shown in Figure 6, the surfaces of all the cement pastes pre-cured at 20 °C and then eroded by sulfate solution for 180 d are damaged. Moreover, with the incorporation of 20~60 wt% DM into blended PC, the appearances become more and more worse. According to Figure 17, the inner structure of the PC-DM pastes is also damaged seriously by sulfate erosion. The erosion products including ettringite and gypsum are observed in the surface and inner portions of the PC paste, and the diffraction peaks of ettringite and gypsum increase obviously with the incorporation of DM, as is shown in Figure 15. This result is mainly due to that the incorporation of DM degrades the pore structure and increases the total porosities according to Figures 12 and 14. The poor pore structure and high porosity accelerate the penetration of SO_4^{2-}, and then SO_4^{2-} reacts with monosulfate and portlandite to increase the amount of ettringite and gypsum, thus resulting in the worse sulfate resistance of the PC-DM pastes.

Additionally, all the cement mortars exhibit slight and slow expansion in the early period and large expansion in the later period. This can be ascribed to that the pressure of ettringite crystallization acts a key role in sulfate attack[2,35,36]. The initial formation of ettringite in large pores does not lead to the obvious deformation, which corresponds to the slight and slow expansion in the early period. With the continuous invasion of SO_4^{2-}, ettringite is formed in small pores, causing the larger expansion in the later period. When DM is incorporated into blended PC, the ingress of external SO_4^{2-} becomes much easier attributed to the high porosity and poor pore structure, thereby leading to the faster and larger expansion than the PC mortars. However, for the PDC60 mortar, the final expansion value is lower than that of the PDC20 and PDC40 mortars. This may be related to that the incorporation of 60 wt% DM causes the insufficient of aluminate phases in cement pastes and decreases the amount of ettringite, thus mitigating a certain expansion of the PDC60 mortar at the later age.

3.6.2 Sulfate resistance of cement-based materials pre-cured at 60 °C

As is presented in Figures 7 and 9, the cement pastes and mortars containing DM pre-cured at 60 °C and then eroded by sulfate solution for 180 d exhibit the better appearances and lower expansion values than the reference PC paste and mortar. Furthermore, the sulfate resistance properties are improved obviously with increasing the DM content. The result is the opposite of that of cement-based materials containing DM pre-cured at 20 °C. However, as is shown in Figures 13 and 14, the pore structure is still coarsened by the incorporation of DM, and the total porosity is even higher than that of the PC-DM pastes pre-cured at 20 °C. It indicates that the degradation of the pore structure does not act as a major factor for the sulfate resistance of blended cement containing DM pre-cured at 60 °C.

In the case of pre-curing at 60 °C for 28 d, monosulfate and portlandite can be observed in the PC paste obviously. When the PC paste sample is soaked in sulfate solution at 20 °C for 180 d, external SO_4^{2-} can react with monosulfate and portlandite to generate ettringite and gypsum [2], respectively, thus causing the worse sulfate resistance. However, it should be noted that the hydration products of the PC-DM pastes pre-cured at 60 °C for 28 d differ significantly from that of the PC paste. Little or no monosulfate is detected in the PC-DM pastes, and Ht can be found obviously in the PC-DM pastes, even the amount of Ht increases with increasing the DM content. This is mainly due to that high pre-curing temperature accelerates the dissolution of Mg^{2+} from DM particles, and then $Al(OH)_4^-$ in the PC pastes combines preferentially with Mg^{2+} to precipitate Ht due to the lower solubility of Ht [24], which can result in the decomposition of monosulfate. Furthermore, the formation of Ht also

consumes the amount of portlandite in the PC-DM pastes according to literature [32]. When the PC-DM pastes are immersed in sulfate solution, little or no monosulfate can react with SO_4^{2-} to generate ettringite. Therefore, the amount of ettringite decreases largely with increasing the DM content, even no ettringite is observed in the PDC40 and PDC60 pastes. Moreover, it seems that Ht is very stable in sulfate environment, which is in line with the studies of the sulfate resistance in the literatures [37,38]. Previous studies [39-41] have also reported that Ht is a layered double hydroxide, which can bind effectively SO_4^{2-} from surround solution. To sum up, the formation of Ht in the PC-DM pastes has a favorable association with improving the sulfate resistance. Additionally, a certain amount of brucite is found in the PDC40 and PDC60 pastes. This may be due to that all Al in the blended cement pastes with high-volume DM has been transformed into Ht, and then the remaining DM begins to react with portlandite to form brucite [42].

4. Conclusions

(1) The cement pastes and mortars containing DM pre-cured at 20 °C and then eroded by sulfate solution for 180 d exhibit the worse appearances and higher expansion values than the reference PC paste and mortar. This is mainly due to that the incorporation of high-volume DM coarsens the pore structure and increases the porosity. The poor pore structure and high porosity accelerate the invasion of SO_4^{2-}, and promote the generation of ettringite and gypsum, thus resulting in the worse sulfate resistance.

(2) When pre-curing is made at 60 °C for 28 d, the degradation of the pore structure due to the incorporation of high-volume DM does not increase the risk of sulfate erosion. On the contrary, the cement pastes and mortars containing high-volume DM exhibit the better appearances and lower expansion values than the reference PC paste and mortar due to the formation of Ht. Additionally, brucite can be identified in the PC-DM pastes pre-cured at 60 °C, especially with high DM dosages.

Acknowledgements

This work is supported by the National Natural Science Foundation of China (52208279, 52102018), Natural Science Foundation of Jiangsu Province of China (BK20220639), Natural Science Foundation of the Jiangsu Higher Education Institution of China (20KJB560007), and the Open Research Program of Anhui Province Key Laboratory of Advanced Building Materials (JZCL006KF).

REFERENCES

[1] A. Neville, The confused world the sulfate attack on concrete, Cement and Concrete Research, 2004, **34**(8),1275.

[2] K. Liu, M. Deng, L. Mo, J. Tang, Deterioration mechanism of Portland cement paste subjected to sodium sulfate attack, Advances in Cement Research, 2015, **27**(8), 477.

[3] M. Hu, F. Long, M. Tang, The thaumasite form of sulfate attack in concrete of Yongan dam, Cement and Concrete Research, 2006, **36**(1), 2006.

[4] B. Ma, X. Gao, E.A. Byars, Q. Zhou, Thaumasite formation in a tunnel of Bapanxia dam in western China, Cement and Concrete Research, 2006, **36**(4), 716.

[5] H. Lee, R.D. Cody, A.M. Cody, P.G. Spry, The formation and role of ettringite in Iowa highway concrete deterioration, Cement and Concrete Research, 2005, **35**(2), 332.

[6] M.M.A Elahi, C.R. Shearer, A.N.R. Reza, A.K. Saha, M.N.N. Khan, M.M. Hossain, P.K. Sarker, Improving the sulfate attack resistance of concrete by using supplementary cementitious materials (SCMs): a review, Construction and Building Materials, 2021, **281**, 122628.

[7] Z. Tang, W. Li, G. Ke, J. Zhou, V.W.Y. Tam, Sulfate attack resistance of sustainable concrete incorporating various industrial solid wastes, Journal of Cleaner Production, 2019, **218**, 810.

[8] R. Khatri, V. Sirivivatnanon, J. Yang, Role of permeability in sulphate attack. Cement and Concrete Research, 1997, **27**(8):1179.

[9] J.W. Sun, Z.H. Chen. Influences of limestone powder on the resistance of concretes to the chloride ion penetration and sulfate attack, Powder Technology, 2018, **338**, 725.

[10] C. Jiang, L. Yu, X. Tang, H. Chu, L. Jiang, Deterioration process of high belite cement paste exposed to sulfate attack, calcium leaching and the dual actions, Journal of Materials Research and Technology, 2021, **15**, 2982.

[11] O.S.B. Al-Amoudi, Attack on plain and blended cements exposed to aggressive sulfate environments. Cement and Concrete Composites, 2002, **24**(3-4), 305.

[12] M.C.G. Juenger, R. Snellings, S. Bernal, Supplementary cementitious materials: New sources, characterization, and performance insights, Cement and Concrete Research, 2019, **122**, 257.

[13] J.D. Brito, R. Kurda, The past and future of sustainable concrete: A critical review and new strategies on cement-based materials, Journal of Cleaner Production, 2021, **281**, 123558.

[14] Z. He, S. Du, D. Chen, Microstructure of ultra high performance concrete containing lithium slag, Journal of Hazardous Materials, 2018, **353**, 35.

[15] A. Machner, M. Zajac, M.B. Haha, K.O. Kjesllsen, M.R. Geiker, K.D. Weerdt, Portland metakaolin cement containing dolomite or limestone-similarities and differences in phase assemblage and compressive strength, Construction and Building Materials, 2017,**157**, 214.

[16] D. Chen, Z. He, A. Wang, T. Yang, Influences of light-burnt dolomite on strength and deformation of blended cement, Revista Română de Materiale / Romanian Journal of Materials, 2021, **51**(1),116.

[17] M. Szybilski, W.N. Wczelik, The effect of dolomite additive on cement hydration, Procedia Engineering, 2015,**108**, 193.

[18] D. Chen, T. Yang, K. Liu, A. Wang, Influence of dolomite powder fineness on hydration of blended cements at different curing temperature, Revista Română de Materiale / Romanian Journal of Materials, 2021, **51**(3), 395.

[19] S. Barbhuiya, Effects of fly ash and dolomite powder on the properties of self-compacting concrete, Construction and Building Materials, 2011, **25**(8), 3301.

[20] H.A. Nguyen, T.P. Chang, J.Y. Shih, H.S. Djayaprabha, Enhancement of low-cement self-compacting concrete with dolomite powder, Construction and Building Materials, 2018, **161**, 539.

[21] S. Krishnan, S. Bishnoi, Understanding the hydration of dolomite in cementitious systems with reactive aluminosilicates such as calcined clay, Cement and Concrete Research, 2018, **108**, 116.

[22] J. Xu, D. Lu, S. Zhang, K. Ling, Z. Xu, Strength and hydration products of cement mortars with dolomite powders cured at 40 °C and 60 °C, Journal of The Chinese Ceramic Society, 2016, **44**(11), 1588.
[23] M. Zajac, S.K. Bremseth, M. Whitehead, B.M. Haha, Effect of $CaMg(CO_3)_2$ on hydrate assemblages and mechanical properties of hydrated cement pastes at 40 ºC and 60 ºC, Cement and Concrete Research, 2014, **65**, 21.
[24] J. Xu, D. Lu, S. Zhang, Z. Xu, R.D. Hooton, Reaction mechanism of dolomite powder in Portland-dolomite cement, Construction and Building Materials, 2021, **270**, 121375.
[25] A. Machner, M. Zajac, B.M. Haha, K.O. Kjellsen, M.R. Geiker, D.K. Weerdt, Stability of the hydrate phase assemblage in Portland composite cements containing dolomite and metakaolin after leaching, carbonation, and chloride exposure, Cement and Concrete Composites, 2018, **89**, 89.
[26] A. Machner, M. Zajac, B.M. Haha, K.O. Kjellsen, M.R. Geiker, D.K. Weerdt, Chloride-binding capacity of hydrotalcite in cement pastes containing dolomite and metakaolin, Cement and Concrete Research, 2018, **107**,163.
[27] J. Lu, A. Xu, J. Xu, D. Lu, Z. Xu, Sulfate resistance of Portland dolomite cement: performance and mechanisms, Materials and Structures, 2020, **53**, 125.
[28] K. Ling, D. Lu, J. Xu, S. Zhang, Z. Xu, Sulfate resistance of Portland cement mortars with dolomite powders, Journal of The Chinese Ceramic Society, 2018, **46**(2), 224.
[29] M. Fourmentin, P. Faure, S. Rodts, U. Peter, D. Lesueur, D. Daviller, P. Coussot, NMR observation of water transfer between a cement paste and a porous medium, Cement and Concrete Research, 2017, **95**, 56.
[30] F. Dalas, J.P. Korb, S. Pourchet, A. Nonat, D. Rinaldi, M. Mosquet, Surface relaxivity of cement hydrates, The Journal of Physical Chemistry C, 2014, **118**, 8387.
[31] B. Lothenbach, T. Matschei, G. Möschner, F.P. Glasser, Thermodynamic modeling of the effect of temperature on the hydration and porosity of Portland cement, Cement and Concrete Research, 2008, **38**, 1.
[32] A. Machner, M. Zajac, B.M. Haha, K.O. Kjellsen, M.R. Geiker, D.K. Weerdt, Limitations of the hydrotalcite formation in Portland composite cement pastes containing dolomite and metakaolin, Cement and Concrete Research, 2018,**105**, 1.
[33] K. Yanagisawa, X. Hu, A. Onda, K. Kajiyoshi. Hydration of β-dicalcium silicate at high temperatures under hydrothermal conditions, Cement and Concrete Research, 2006, **36**, 810.
[34] P.K. Mehta, P.J.M. Monteiro, Concrete: microstructure, properties, and materials. New York: McGraw-Hill, 2006.
[35] G.W. Scherer, Stress from crystallization of salt, Cement and Concrete Research, 2004, 34(9), 1613.
[36] C. Yu, W. Sun, K. Scrivener, Mechanism of expansion of mortars immersed in sodium sulfate solutions, Cement and Concrete Research, 2013, **43**, 105.
[37] M. Komljenović, Z. Baščarević, N. Marjanović, V. Nikolić, External sulfate attack on alkali-activated slag, Construction and Building Materials, 2013, **49**, 31.
[38] X. Yan, L. Jiang, M. Guo, Y. Chen, Z. Song, R. Bian, Evaluation of sulfate resistance of slag contained concrete under steam curing, Construction and Building Materials, 2019, **195**, 231.
[39] Y. Chen, R. Yu, X. Wang, J Chen, Z. Shui, Evaluation and optimization of ultra-high performance concrete (UHPC) subjected to harsh ocean environment: towards an application of layered double hydroxides(LDHs), Construction and Building Materials, 2018, **177**, 51.
[40] P. Duan, C. Yan, W. Zhou, Effects of calcined layered double hydroxides on carbonation of concrete containing fly ash, Construction and Building Materials, 2018, **160**, 725.
[41] L. Guo, Y. Wu, P. Duan, Z. Zhang, Improving sulfate attack resistance of concrete by using calcined Mg-Al-CO3 LDHs: Adsorption behavior and mechanism, Construction and Building Materials, 2020, **232**,117256.
[42] E, García, P, Alfonso, M, Labrador, S. Galí, Dedolomitization in different alkaline media: application to Portland cement concrete, Cement and Concrete Research, 2003, **33**,1443.

****